Active Site Structure in Cytochrome *c* Peroxidase and Myoglobin Mutants: Effects of Altered Hydrogen Bonding to the Proximal Histidine

R. Sinclair,[‡] S. Hallam,[‡] M. Chen,[‡] B. Chance,[§] and L. Powers*,[‡]

National Center for the Design of Molecular Function, Utah State University, Logan, Utah 84322-4630, and Department of Biochemistry and Biophysics, University of Pennsylvania Medical School, Philadelphia, Pennsylvania 19104

Received May 3, 1996; Revised Manuscript Received August 21, 1996[⊗]

ABSTRACT: The globins and peroxidases, while performing completely different chemistry, share features of the iron heme active site: a protoporphyrin IX prosthetic group is linked to the protein by the proximal histidine residue. X-ray absorption spectroscopy provides a method to determine the local structure of iron heme active sites in proteins. Our previous studies using X-ray absorption spectroscopy revealed a significant difference in the Fe−N_ϵ bond length between the peroxidases and the globins [for a review, see Powers, L. (1994) *Molecular Electronics and Molecular Electronic Devices*, Vol. 3, p 211 CRC Press Inc., Boca Raton, FL]. Globins typically have an Fe−N_ϵ distance close to 2.1 Å while the Fe−N_ϵ distance in the peroxidases is closer to 1.9 Å. We have proposed [Sinclair, R., Powers, L., Bumpus, J., Albo, A., & Brock, B. (1992) *Biochemistry 31*, 4892] that strong hydrogen bonding to the proximal histidine is responsible for the shorter bond length in the peroxidases. Here we use site-specific mutagenesis to eliminate the strong proximal hydrogen bonding in cytochrome *c* peroxidase and to introduce strong proximal hydrogen bonding in myoglobin. Consistent with our hypothesis, elimination of the Asp235−His175 hydrogen bond in CcP results in elongation of Fe−N_ϵ from ∼1.9 to ∼2.1 Å. Conversely, introduction of a similar strong proximal hydrogen bond in myoglobin shortens Fe−N_ϵ from ∼2.1 to ∼1.9 Å. These results correlate well with other biochemical data.

The iron heme peroxidases comprise an extremely important group of biocatalysts which perform substrate oxidations coupled with the coordinate consumption of hydrogen peroxide. Their current use in biosensors and clinical and biochemical assays, their potential use in biomolecular devices, and the biodegradation of environmental xenobiotics are a few examples of their broad utility. Despite decades of intensive study of numerous hemeproteins, the effects of the protein on the structure of the heme and the relationship between heme structure and overall reactivity remain elusive. The use of high-resolution structural tools, such as X-ray absorption spectroscopy (XAS),[1] coupled with recombinant DNA approaches offers a unique investigation into these relationships.

X-ray absorption spectroscopy can provide information about the local environment of the heme iron in hemeproteins such as globins and peroxidases. The extended X-ray absorption fine structure (EXAFS) region contains information about the number and average distance of ligands and their relative disorder. Not only can differences in Fe−ligand bond lengths be determined to ±0.015 Å, but the relative position of the iron with respect to the heme plane can be investigated (Powers et al., 1981, 1984; Chance et al., 1986a). Thus, this method offers a sensitive comparison of the active sites of the hemeproteins including their reactive intermediates and liganded states (Chance et al., 1984, 1986b,c).

Several peroxidases have received extensive attention due to their potential applications (the lignin peroxidases of *Phanerochaete chrysosporium*; LiP) or their historical significance (horseradish peroxidases; HRP). While cytochrome *c* peroxidase (CcP) has no major commercial application, it has become the model protein for heme peroxidase research. The spectral, kinetic, and structural analyses performed on the native protein and its H_2O_2-activated intermediate, compound ES, provide a basis for understanding the structure−function relationship in peroxidases. Many of these studies revealed similarities to HRP (Yonetani, 1965), but differences were also reported. Unlike HRP compound I, which is known to be a ferryl iron heme cation radical, CcP compound ES is a ferryl species with a radical on Trp191 (Yonetani et al., 1966b; Yonetani, 1970; Sivaraja et al., 1989). Much of the research focus has been due to the early publication of an X-ray crystal structure (Finzel et al., 1984; Poulos & Finzel, 1984). A more recent structure (Pelletier & Kraut, 1992) shows details of the CcP−cytochrome *c* complex, suggesting a likely electron transfer path.

One significant feature of the CcP crystal structure is the presence of strongly hydrogen-bonding proximal histidine (Peisach, 1975; Finzel et al., 1984). In CcP, the side-chain carboxylate of Asp235 is H-bonded to both Trp191 and His175, the proximal ligand of the heme iron. It has been proposed that this strong proximal hydrogen bonding controls heme reactivity (Peisach, 1975; Finzel et al., 1984). The strong H-bond is believed to result in increased electron density on the histidine imidazole−Fe−porphyrin system,

[‡] Utah State University.
[§] University of Pennsylvania Medical School.
[⊗] Abstract published in *Advance ACS Abstracts,* November 15, 1996.
[1] Abbreviations XAS, X-ray absorption spectroscopy; Mb, myoglobin; SWMb, sperm whale myoglobin; HHMb, horse heart myoglobin; CcP, cytochrome *c* peroxidase; EXAFS, extended X-ray absorption fine structure; wt, wild-type protein; LiP, lignin peroxidases; HRP, horseradish peroxidases; Fe−N_p, iron-to-heme pyrrole nitrogen average distance; Fe−N_ϵ, iron-to-proximal histidine nitrogen distance; Fe−X, iron-to-distal ligand distance; Fe−ct, distance iron is out of the average heme plane.

S0006-2960(96)01064-1 CCC: $12.00 © 1996 American Chemical Society

which would aid in stabilizing both the heme and radical electron-deficient centers that exist in compound ES. Several studies have been published that agree with this idea (Mincey & Traylor 1979; Traylor & Popovitz-Biro, 1988; Fujita et al., 1983). Strong proximal H-bonding might therefore be expected to be a general feature of the heme peroxidases in general. Alignment of the amino acid sequences of a number of plant and fungal heme peroxidases reveals candidates for CcP Asp235 equivalents in most cases (Henrissat et al., 1990; Sinclair & Hallam, unpublished data), and recent crystal structures confirm this (Poulos et al., 1993; Kunishima et al., 1994; Fenna et al., 1995; Schuller et al., 1996). Additionally, proton NMR studies of HRP (deRopp et al., 1985; LaMar & deRopp, 1982) show this enzyme also has an important proximal proton acceptor. This residue was proposed to also be an aspartic acid, Asp247 in HRP isoenzyme E, in keeping with deductions from CcP.

While CcP provides a basis for understanding the heme peroxidases, myoglobin (Mb), the oxygen transport protein found in muscle tissue, provides another opportunity for the study of heme−protein interactions. The heme in Mb is chemically identical (i.e., a *b*-type heme) to the peroxidase heme and is bonded to the protein in an identical manner via a proximal histidine residue. Therefore, the radically different chemistry performed by these two proteins must be controlled by the surrounding protein.

The myoglobin heme pocket differs from CcP in two important ways. First, Mb lacks the distal His-Arg pair essential for efficient peroxide cleavage (Poulos & Kraut, 1980; Finzel et al., 1984). Second, the strong proximal hydrogen-bonding network involving CcP His175, Asp235, and Trp191 is missing. In Mb, a much weaker proximal hydrogen-bonding network is found which involves the proximal ligand (His93), the side chain of Ser92, and a backbone carbonyl of Leu89.

A sperm whale Mb (SWMb) gene with optimal codon usage for *Escherichia coli* has been synthesized, cloned in *E. coli* as plasmid pMb413a, and efficiently expressed as the holoprotein (Springer & Sligar, 1987). This, and similar expression systems, have been used to introduce specific changes in various Mbs (e.g., human (Adachi et al., 1993), horse heart (Guillemette et al., 1991), and pig (Smerdon et al., 1993)). A number of mutants of the distal histidine residue (MbHis64) of SWMb have been prepared, primarily to analyze ligand binding [e.g., Stayton et al. (1989)]. The gene for horse heart Mb (HHMb) has recently been cloned in *E. coli* (Guillemette et al., 1991) and used for site-directed mutagenesis (Reddy et al., 1992). We have recently performed XAS studies on a distal histidine-to-tyrosine replacement (MbH64Y) in HHMb. At pH 7, the tyrosine is directly coordinated to the heme iron as the distal ligand, while at pH 4.2, a water replaces the tyrosine at the distal position. These structures correlate well with observed reactivity: at neutral pH, weak ligands like CN^- and azide slowly displace the tyrosine ligand, while at pH 4.2, CN^- and azide can bind rapidly although some differences were observed compared to wild type (Tang et al., 1994).

Mb is not generally considered to be a peroxidase; however, the ferric form can react comparatively slowly with hydrogen peroxide to form a Mb peroxide species analogous to peroxidase compound II in that it contains a single oxidizing equivalent above the met form (George & Irvine, 1952, 1953; Yonetani & Schleyer, 1967). The second oxidizing equivalent from the peroxide is rapidly transferred from the heme center to form a protein radical (Harada & Yamazaki, 1987; Miki et al., 1989) based on Tyr103 (Davies, 1990, 1991; Tew & Ortiz de Montellano, 1988). In this respect, it is very similar to compound ES of CcP. Mb appears to use its own amino acid side chains as substrate as it is progressively modified by this reaction until, after ∼8 cycles, it can no longer react with hydrogen peroxide (King & Winfield, 1963). Recent studies have shown that met SWMb dimerizes upon reaction with H_2O_2 by means of a cross-link between Tyr103 and Tyr151 (Tew & Ortiz de Montellano, 1988).

Our studies over the past several years have revealed consistent differences between the structure of the heme in the globins and peroxidases [for a review see Powers (1994)]. Globins typically have an iron-to-proximal nitrogen distance ($Fe-N_\epsilon$) of ∼2.1 Å while in the peroxidases this distance is typically shorter by ∼0.2 Å, resulting in a typical $Fe-N_\epsilon$ distance of ∼1.9 Å (Chance et al., 1984, 1986b,c; Sinclair et al., 1992, 1995; Chang et al., 1993a,b; Powers et al., 1994; Powers, 1994). The CcP heme is a typical peroxidase in this respect (Chance et al., 1984). In fact, the heme structure of CcP is very similar to that of HRP, CcP exhibiting an $Fe-N_\epsilon$ distance of 1.94 Å, iron-to-heme pyrrole nitrogen average distance ($Fe-N_p$) of 2.05 Å and iron-to-distal ligand distance (Fe−X) of 2.3 Å. Further, CcP compound ES, despite known differences in location of the radical, has an active site structure almost identical to HRP compound I ($Fe-N_\epsilon$ of 1.91 Å, $Fe-N_p$ of 2.02 Å and Fe−X of 1.67 Å (Chance et al., 1986c)). While one functional significance of strong proximal hydrogen bonding in the peroxidases is stabilization of the electron-deficient centers that exist in compound I, it is also likely the strong proximal H-bonding is directly responsible for the shorter $Fe-N_\epsilon$ distance, due to redistribution of the electron density around the heme iron (Peisach, 1975; Valentine, et al., 1979; Finzel et al., 1984; Sinclair et al., 1992). The globins, typified by SWMb, lack this strong hydrogen bonding to the proximal histidine and exhibit a longer $Fe-N_\epsilon$ bond.

In addition to shortening the $Fe-N_\epsilon$ bond, Asp235 and Trp191 have other potential roles. One is that Trp191 forms part of an H-bonding network whose function is to optimally position and orient Asp235 for H-bonding to the proximal histidine. This results in regulation of the $Fe-N_\epsilon$ bond strength and prevention of Fe movement into the heme plane (Smulevich et al., 1990a) which, in turn, regulates the reduction potential. Alternatively, the hydrogen-bonding network, including the bond from Asp235, functions to maintain an optimal position and orientation of Trp191 (Wang et al., 1990; Goodin & McRee, 1993). This optimal orientation allows formation of the compound ES radical on Trp191 and possibly facilitates a weak exchange interaction and electron transfer between CcP-ES and cytochrome *c*.

Disruption of the Asp235−His175 H-bond by a D235N mutation resulted in a lower $Fe-N_\epsilon$ stretching frequency and a change in coordination to a mixed-spin aquo complex in the ferrous state (Smulevich et al., 1988a). In the 6-coordinate form, a weakened $Fe-N_\epsilon$ allows the Fe to move more into the heme plane, resulting in direct iron coordination from a pocket water molecule (H_2O595) at a distance of ∼2 Å (Smulevich et al., 1990b; Wang et al., 1990). Additionally, the ring of Trp191 rearranges in this mutant to form a new H-bond with Leu177. These studies suggest the Asp235−

His175 H-bond could keep the Fe−N_ϵ bond short, pulling the Fe out of the heme plane and maintaining a pentacoordinate state. This vacancy of the distal position probably results in increased reaction rate with H_2O_2 (Wang et al., 1990). This role in heme reactivity for Asp235 is in addition to those proposed by Smulevich et al. (1991), who suggested the proximal H-bonding, by modulating the donor strength of the imidazolate axial ligand, assists with the heterolytic cleavage of H_2O_2 (Poulos & Kraut, 1980) and promotes dissociation of the leaving H_2O.

The experiments described herein focus on whether the strong and weak proximal hydrogen-bonding network in CcP and SWMb, respectively, are directly responsible for the differences in Fe−N_ϵ bond lengths. D235N and W191F mutants of CcP have previously been constructed (Smulevich et al., 1988), which allow us to investigate whether the disruption of the strong proximal hydrogen-bonding network in CcP results in a longer (globin-like) Fe−N_ϵ bond. Our molecular modeling studies of SW myoglobin (Sinclair & Hallam, unpublished) suggested there is sufficient flexibility in this region to replace Leu89 with aspartic acid and to allow side-chain hydrogen bonding from Asp89 to the proximal histidine.

EXPERIMENTAL PROCEDURES

Construction of Myoglobin Mutants. pMb413a (pUC19 containing the cloned synthetic gene for SWMb (Springer & Sligar, 1987)) was digested with *Sph*I and *Pst*I to remove the 312 bp fragment of the SWMb gene. PCR amplification (using *Taq* polymerase (New England Biolabs) and a DNA thermal cycler (Perkin-Elmer Cetus)) of the 312 bp fragment from the intact SWMb gene between the *Sph*I and *Pst*I sites was achieved using the M13 reverse primer and the oligonucleotide

5′-AGTAGCATGCGATTGCGCT(A)T(A)T(C)
GGTTT*GAGCTC*AGC- 3′

The position where two nucleotides are shown (second in parentheses) indicates an either/or situation resulting in six possible sequences. The region in italics is the *Sph*I site. The population of DNA from the PCR reaction was digested with *Sph*I and *Pst*I. Both the *Sph*I- and *Pst*I-digested pMb413a and the amplified fragment were gel-purified from 1.2% agarose using a Geneclean II kit (Bio 101). The pMb413a material and amplified fragment were then ligated together. The ligated DNA was used to transform *E. coli* strain TB1, and resulting colonies were screened by dideoxy sequencing of double-stranded DNA. A clone was selected for each required mutational change and sequenced throughout the entire *Pst*I to *Sph*I fragment and junctions to confirm the absence of secondary mutations. Use of the mixed oligonucleotide shown above for the PCR amplification gave site-specific mutation of the Leu89 residue to Ile, Val, Asp, Asn, Lys, or Glu (MbL89I, MbL89V, and MbL89D, respectively). Each clone, selected on the basis of the dideoxy sequence screening, was also assessed for myoglobin production by SDS−PAGE of a crude cell lysate from representative colonies. Standard molecular biology procedures were as described by Sambrook et al. (1989).

Sample Preparation. L89I, L89V, and wt Mbs were purified as described by Springer and Sligar (1987). The L89D protein was found to be less stable than wt Mb and was therefore purified by a modification of this procedure. The crude lysate was stirred at 4 °C with an approximate molar equivalent of hemin for 4−12 h to convert apoprotein to holoprotein. In addition, the anion exchange step was omitted from the procedure to reduce a significant loss of protein at this stage, and the cation exchange column was equilibrated to pH 6.7. It is not possible to reconstitute the protein with hemin after purification because of the difficulty with removing the excess hemin. (Extraneous iron in the protein preparation would render it useless for XAS studies.) At each stage of the purification, purity was evaluated using optical spectroscopy and SDS−PAGE. Native SWMb was purchased from Sigma before the ban on whale products. We further purified this material according to Powers et al. (1987). Globin samples were concentrated to ∼1−4 mM in 0.1 M potassium phosphate buffer (pH 6.8).

Protein samples of CcPMI, CcPD235N, and CcPW191F were a gift from Dr. M. Miller and Dr. J. Kraut and were provided as crystals in water. We collected the crystals by centrifugation and resuspended them to a protein concentration of 2−4 mM in 0.1 M potassium phosphate buffer, pH 6.8. The XAS samples contained 40% (v/v) ethylene glycol as a cryoprotectant and were stored in the dark in liquid nitrogen before and after XAS data collection. We examined optical spectra before and after XAS data collection to evaluate sample damage. Due to difficulties inherent in assaying the CcP mutants for activity (M. Miller, personal communication), we did not evaluate protein activity following X-ray exposure.

Data Collection and Analysis. EXAFS fluorescence data were recorded at the Stanford Synchrotron Radiation Laboratory beam lines IV-3 and VI-2 (Stanford, CA) and the National Synchrotron Light Source beam line X-9 (Brookhaven, NY) using a phosphorescent phototube detector (Khalid et al., 1986). The beam line monochromators were equipped with Si(111) crystals providing 2−3 eV resolution at the Fe K-edge. Except where noted, experiments were carried out at ∼−100 °C to prevent conversion to the native form by hydrated electrons produced by X-ray exposure (Chance et al., 1980).

The ligand field indicator ratio (LFIR) was calculated according to Chance et al. (1984). The XAS data were analyzed by procedures described previously (Powers et al., 1981, 1984; Lee et al., 1981). Data from each light source were analyzed separately before combination. Background subtraction was followed by k^3 multiplication and normalization to one absorbing atom where k is the photoelectron wave vector. The final EXAFS modulations are shown in Figure 1. These EXAFS modulations were then Fourier transformed as shown in Figure 2. The first shell peak of the Fourier transform was Fourier filtered and back-transformed. Similar data for three model compounds, Fe^{3+}−bis(imidazole-tetraphenylporphinato) chloride (Collins et al., 1972), Fe^{2+}−acetylacetonate, and Fe^{3+}−acetylacetonate (Iball & Morgan, 1976) were collected under identical conditions and analyzed using the procedures described above. The filtered data were then fitted with that of the model compounds using a two-atom-type fitting procedure. Each atom type in the fitting procedure is represented by an average distance (r), an amplitude factor containing the number of ligands (N), a change in Debye−Waller factor ($\Delta\sigma^2 = \sigma^2_{\text{model}} - \sigma^2_{\text{enzyme}}$), and a change in threshold energy ($\Delta E_o = E_{\text{omodel}} - E_{\text{oenzyme}}$). Since the amplitude factor is highly correlated with $\Delta\sigma^2$, the

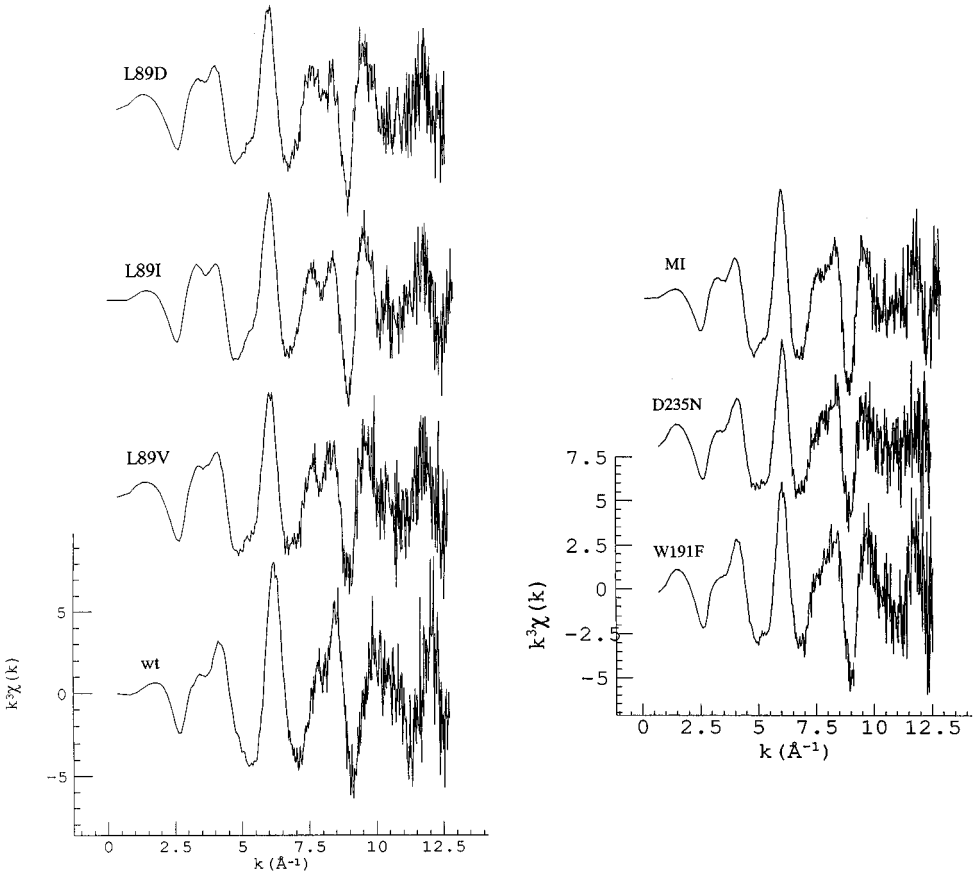

FIGURE 1: Background-subtracted, k^3-multiplied EXAFS data normalized to one absorbing atom for Mb (left) and CcP (right).

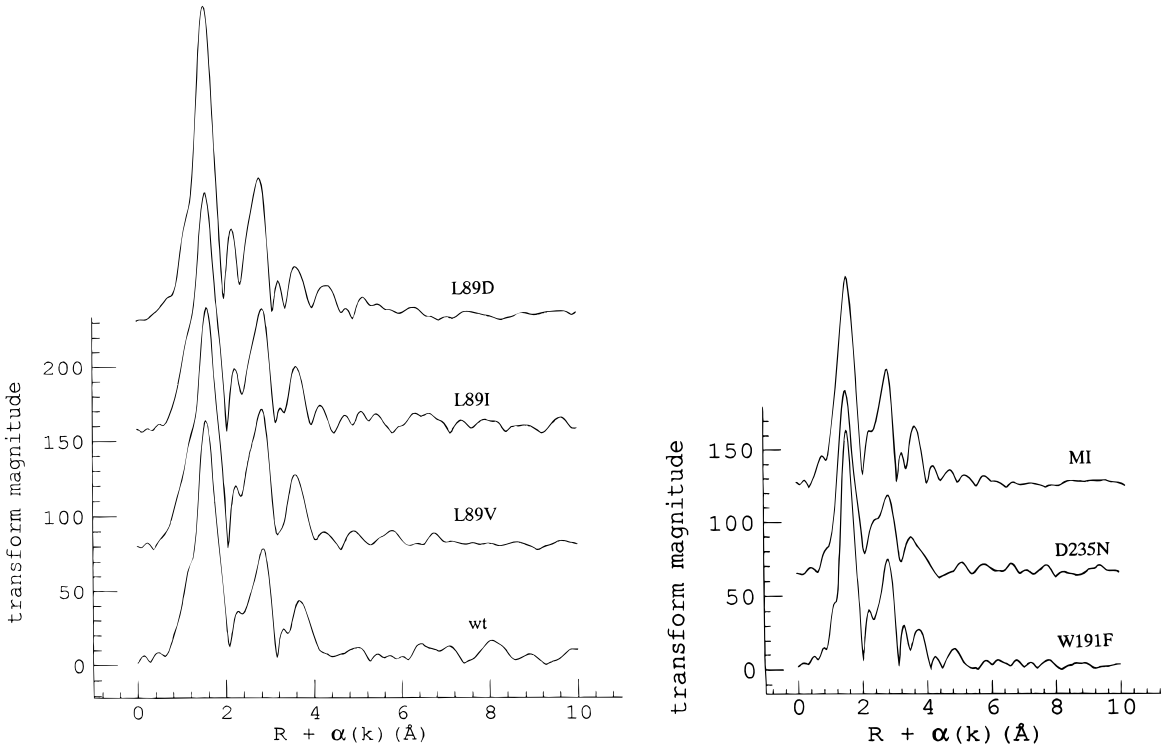

FIGURE 2: Fourier transforms of the EXAFS data of Figure 1: Mb (left) and CcP (right).

N parameters were held fixed at their known values (Peisach et al., 1982). Several possible solutions were judged to be statistically different only if the $\Sigma R^2 > \Sigma R^2_{min}(1 + 1/\phi_f)$, where ΣR^2_{min} is the minimum sum of residuals squared for a physically reasonable solution, $\phi_f = \phi_d - p$, where p is the number of variables in the fit, and ϕ_d is the number of degrees of freedom in the filtered data. The variable ϕ_d was estimated by $2\Delta w \Delta k/\pi$, where Δw is the full width at half-maximum of the filter window and Δk was the length of the data used. After possible solutions were found for each contribution to the first shell (Fe−N_p, Fe−X, Fe−N_ϵ), a three-atom-type consistency test was carried out using all

three sets of scatterers with r and N held constant in order to verify that the three distances actually coexist in the data. The ΣR^2 for the three-atom consistency test must be smaller than those obtained for the two atom-type solutions. To ensure that the three distances obtained from the above steps constitute a true minimum, each distance was allowed to vary individually. In each case, the residuals of the consistency test were comparable to the estimated error over the entire k range.

Total error for each distance was determined by changing the parameter to a different value while holding all other parameters constant until the sum of the $\sum R^2$ increased by a factor of 2 on each side of the minimum. A detailed discussion of analysis error is given by Powers and Kincaid (1989).

The higher-order shells result largely from contributions of the rigid heme structure and a contribution from the rigid imidazole structure of the proximal histidine. A group site-modeling approach (Powers & Kincaid, 1989; Powers et al., 1981) based on these contributions was used to determine which axial distance belonged to the proximal histidine. The second through fifth partially resolved heme outer shells were modeled by those of tetraphenylporphyrin (TPP) as a group. Similarly, the second and third shells of histidine imidazole were modeled as a group by those of tetraimidazole. A two-atom-type fitting procedure was then used to fit the second through fifth partially resolved outer shells of the proteins using these groups. If the average Fe−N_p heme distance in the protein was longer or shorter than that of the model, then the fitted average distance for the TPP group was longer or shorter by the same amount. Similarly, the average imidazole group fitted distance identified which axial ligand distance belonged to histidine.

RESULTS

DNA sequence analysis identified clones which contained the desired changes in the SWMb gene. SDS−PAGE analysis of crude lysates from a selection of clones revealed adequate expression of protein from wt Mb, MbL89I, and MbL89V while expression from MbL89D was less efficient. Large-scale purification of MbL89I and MbL89V proceeded as previously observed for wt Mb and resulted in large amounts of essentially pure protein. Purification of MbL89D, even with modifications to the protocol described in the Materials and Methods section, was problematical. Two peaks were collected from the cation exchange column, one essentially brown and a second essentially red. Optical absorption spectroscopy showed these to be met and oxy forms, respectively. The yield of MbL89D was also extremely poor, necessitating conversion of the oxy form to met by titration with hexachloroiridate and pooling of the samples prior to XAS sample preparation. Finally, due to omission of the anion exchange step in the protocol, the MbL89D sample was likely contaminated with other proteins. However, the optical absorption spectra were comparable to that of wt SWMb, and XAS and EPR spectroscopy suggested little contamination with extraneous iron in the MbL89D sample.

The three recombinant CcP preparations, CcPMI, CcPD235N, and CcPW191F, were all bright red at liquid nitrogen temperature indicative of 6-coordinate (hydroxide liganded) low-spin heme (Smulevich et al., 1989; Vitello et al., 1992). Wt CcP, purified from yeast, is also in this form under these conditions. Optical spectroscopy of the preparations indicated highly pure protein preparations.

Table 1: Summary of Results for Wild Type CcP and SWMb and Their Respective Mutant Forms

	LFIR (±0.05)	Fe−ct (Å) (±0.3 Å)	Fe−N_p (Å) (±0.015 Å)	Fe−N_ϵ (Å) (±0.02 Å)	Fe−X (Å) (±0.05 Å)
CcP MI	1.20	0.4	2.04	1.93	2.11
CcP D235N	1.21	0.4	2.03	2.12	1.93
CcP W191F	1.13	0.4	2.01	1.93	2.13
Mb-N	1.3	0.45	2.045	2.14	1.97
Mb-L89I	1.21	0.4	2.035	2.13	1.97
Mb-L89V	1.28	0.45	2.05	2.28	1.98
Mb-L89D					
−100 °C	1.0	0.3	1.985	1.92	2.08
−75 °C	1.0	0.3	1.98	1.91	2.06
−40 °C	1.15	0.4	2.02	1.90	2.35
room temp	1.35	0.45			

Following X-ray exposure, the optical spectra of all proteins except MbL89D were essentially unaltered. While we were unable to evaluate the effects of X-ray exposure on the specific activity of the protein preparations, our other XAS experiments, performed under similar conditions with a wide variety of hemeproteins, suggest that the procedure results in less than 10% damage. However, after X-ray exposure, optical spectroscopy showed MbL89D (met) to be another species, likely a 6-coordinate species. The stability of the MbL89D sample was examined in more detail. Preliminary EPR data suggested a change in spin state upon freezing MbL89D, while optical spectroscopy showed the conversion to a 6-coordinate form. This low-temperature form was investigated at ∼−100, ∼−75, and ∼−40 °C by XAS. However, we were only able to determine the LFIR of MbL89D at room temperature before significant X-ray damage occurred.

Table 1 summarizes the results of the XAS experiments. In the absence of phenomena such as heme-ruffling or twisting, the LFIR parameter is related to the Fe out-of-plane distance (Fe−ct) (Chance, 1986b)

$$\text{Fe−ct} \sim (\text{LFIR}-0.52)/1.7$$

Table 2 summarizes the three-atom-type consistency test results, and Figure 3 illustrates these.

The results for CcPMI show that it is largely a hexacoordinate species at ∼−100 °C. While another solution can also be found with Fe−X ∼2.4 Å, similar to that reported for the wild type by Chance et al. (1984), it does not fit the data as well. This indicates that CcPMI is likely a mixture of the two forms under these conditions (Smulevich et al., 1989). As expected from previous studies on wild type enzyme, the CcPMI proximal histidine, when fitted as a group, is associated with the 1.91 Å axial distance. In SWMb, the proximal histidine is associated with the 2.15 Å distance (Chance et al., 1984; Powers et al, 1984); as expected, this is ∼0.26 Å longer than the value for CcPMI. The histidine in CcPW191F is associated with the 1.93 Å distance, similar to CcPMI, while the histidine in CcPD235N is associated with the 2.12 Å distance, similar to SWMb. All the myoglobin mutants, except MbL89D, have a proximal histidine distance typical of the globins. However, MbL89D shows a proximal histidine distance similar to peroxidases.

Table 2: Three Atom-Type Consistency Tests for the Seven Protein Preparations

	N^a	r (Å)	$\Delta\sigma^2$ (Å^2)	$\Delta E_o{}^b$ (eV)	ΣR^2
CcP	4	2.04	1.5×10^{-3}	2.2	1.7
	1	1.93	3.7×10^{-3}	−2.5	
	1	2.11	3.1×10^{-3}	−3.4	
CCPD235N	4	2.03	3.8×10^{-3}	−1.3	2.4
	1	2.12	5.7×10^{-3}	−0.5	
	1	1.93	6.5×10^{-3}	−2.4	
CcPW191F	4	2.01	5.1×10^{-3}	−0.9	2.0
	1	1.93	5.4×10^{-3}	−5.4	
	1	2.13	7.0×10^{-3}	0.2	
SWMb−N	4	2.045	3.8×10^{-3}	0	1.0
	1	2.15	4.7×10^{-3}	2.1	
	1	1.98	1.6×10^{-3}	1.0	
MbL89I	4	2.035	2.8×10^{-3}	0.4	0.5
	1	2.13	-4.3×10^{-3}	−1.3	
	1	1.97	1.8×10^{-3}	1.4	
MbL89V	4	2.05	3.2×10^{-3}	0.3	0.5
	1	2.28	-1.6×10^{-2}	−3.2	
	1	1.98	7.6×10^{-4}	1.7	
MbL89D					
−100 °C	4	1.985	5.7×10^{-3}	−0.1	2.5
	1	1.92	6.4×10^{-3}	−3.7	
	1	2.08	$8.2 \times 10-3$	3.6	
−75 °C	4	1.98	1.0×10^{-3}	−0.1	1.2
	1	1.91	-9.3×10^{-4}	2.3	
	1	2.06	5.4×10^{-4}	−1.0	
−40 °C	4	2.02	2.3×10^{-3}	0.8	0.7
	1	1.90	6.3×10^{-3}	−1.7	
	1	2.35	-9.0×10^{-3}	−5 .9	

[a] N values fixed, $\Delta\sigma^2$ ($\sigma^2_{\text{model}} - \sigma^2_{\text{enzyme}}$) ±35%. [b] $\Delta E_o = (E_{\text{omodel}} - E_{\text{oenzyme}}) \pm 2.0$ eV.

DISCUSSION

Despite known differences between the sequences of wt CcP and the recombinant enzyme, CcPMI, one form of the enzyme observed under these conditions is identical to the wild type within the error. The dominant form differs only in the distal ligand distance. The two mutant forms of the enzyme do exhibit differences from CcPMI. CcPW191F has a shorter Fe−N_p distance and smaller LFIR while the proximal and distal ligand distances of 1.93 and 2.13 Å, respectively, are similar to CcPMI. CcPD235N has a significantly altered heme structure. The average Fe−N_p distance is very similar to CcPMI, but the axial ligands are significantly different. The proximal ligand has lengthened from 1.91 to 2.12 Å while the distal ligand has shortened from 2.11 (and 2.44) to 1.93 Å. We have fitted the higher coordination shells as group contributions from heme and histidine to determine which axial first coordination shell distance belongs to the proximal histidine.

Our XAS studies of HRP, CcP, and SWMb (Chance et al., 1984, 1986b,c; Powers, 1989) have shown that the Fe−N_ϵ distance is shorter in the peroxidases (∼1.9 Å) compared to the globins (∼2.1 Å). This was proposed to be crucial to the differing reactivity observed between the two groups of proteins (Chance et al., 1984, 1986b,c). Recently, we have extended these studies to a wider range of peroxidases and their liganded and reactive intermediate states, including *P. chrysosporium* lignin and manganese-dependent peroxidases (Sinclair et al., 1992), lactoperoxidase (Chang et al., 1993b), *Coprinus microrhizus* peroxidase, *Arthromyces ramosus* peroxidase, microperoxidase, and several others (Powers, 1994), all of which confirm the shorter Fe−N_ϵ distance in the peroxidases. Further, high-resolution X-ray crystal structures of HHMb and SWMb confirm this trend (Evans & Breyer, 1990; Lionetti et al., 1991). It is therefore not surprising that recombinant CcP has a structure closely resembling wt CcP with a short Fe−N_ϵ distance.

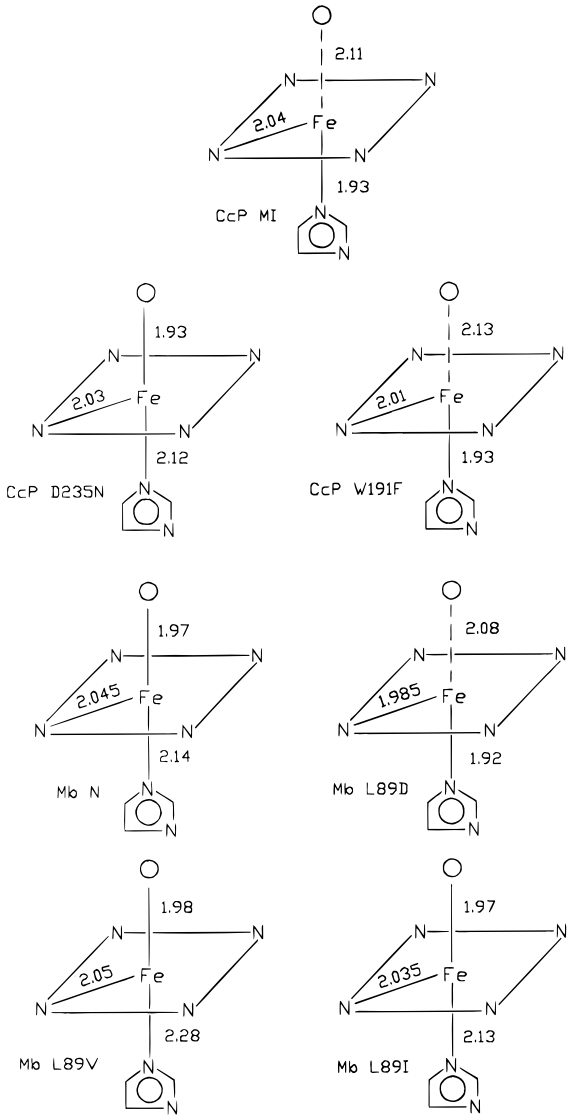

FIGURE 3: Pictorial representation of the XAS results (Tables 1 and 2).

The strong H-bond from D235 to H175 in CcP was proposed to be responsible, at least in part, for the control of heme reactivity (Peisach, 1975; Finzel et al., 1984), for the optimal orientation of W191 in radical formation in compound ES and electron transfer to cytochrome *c* (Wang et al., 1990; Goodin & McRee, 1993; Houseman et al., 1993), and for modulation of the Fe−N_ϵ bond strength and prevention of Fe movement into the heme plane (Smulevich et al., 1990a). We extended this latter hypothesis (Sinclair et al., 1992) to propose that the strong proximal hydrogen bonding is, additionally, responsible for the shorter Fe−N_ϵ bond observed in the peroxidases, probably by causing a redistribution of electron density in the heme proximal histidine system. Disruption of the D235−H175 H-bond through mutagenesis should alter the Fe−N_ϵ bond length. This appears to be the case, as CcPD235N has a proximal bond that is lengthened from 1.91 (peroxidase-like) to 2.12 Å (globin-like) and this mutant possesses a more neutral proximal histidine imidazole ring than wild type or CcPMI (Satterlee et al., 1990).

In addition to the lengthening of the Fe−N_ϵ bond, CcPD235N exhibits other features that are different from CcPMI or wt CcP. Most notable of these is the significantly shortened distal ligand bond length, from 2.11 Å in CcPMI to 1.92 Å in CcPD235N. Smulevich et al. (1990a) proposed that one role of the D235−H175 H-bond is to prevent movement of the Fe into the average heme plane. Therefore, it might be expected that relaxation of that constraint would allow Fe movement into the heme plane (analogous in some ways to T-state hemoglobin), facilitating relatively tight binding of a distal ligand and allowing the distal bond to shorten. If that is the case, we need to explain the unchanged LFIR parameter between CcPMI and CcPD235N, both of which indicate that the Fe is displaced from the average heme plane by ∼0.4 Å. The LFIR parameter is a result of multiple scattering in the XAS experiment and is, therefore, very sensitive to ruffling or twisting of the heme. It is possible that the unchanged LFIR parameter in CcPD235N is a consequence of distortion of the heme. Goodin and McRee (1993) noted that one consequence of the CcPD235N mutation is to cause local changes in the crystal structure, most notably a reorientation of the W191 side chain to form a new H-bond with L177. These local distortions in the heme pocket could easily affect the geometry of the heme. Another possibility is that the CcP heme pocket cannot accommodate a globin-like elongated Fe−N_ϵ bond, and the iron is consequentially forced through the average heme plane to result in displacement to the distal side or that the heme is severely distorted.

Asp235, in addition to forming the strong H-bond with H175 in CcP, forms an H-bond with W191, the likely site of the compound ES radical in native or wild type protein. Two possibilities have been proposed for the role of the D235−W191 H-bond. This H-bond could serve to keep the W191 side chain optimally positioned for radical formation and electron transfer (Wang et al., 1993) and/or could serve to optimally position D235 for H-bonding to H175. CcPW191F exhibits heme changes that indicate that W191 largely serves to position D235 for optimal H-bonding. When the W191−D235 H-bond is disrupted by mutagenesis, temperature-dependent formation of 6-coordinate high-spin heme is observed (Smulevich et al., 1988a, 1990b). Our results show that the CcPW191F mutant retains a peroxidase-like Fe−N_ϵ bond of 1.91 Å. If W191 served to optimally position D235 for H-bonding to H175, this weakened H-bond should lengthen the Fe−N_ϵ distance. Further evidence that the D235−W191 H-bond serves largely to position W191 rather than D235 comes from Fishel et al. (1991), who demonstrated that the W191 radical is absent in compound ES of the CcPD235N mutant.

XAS results for wild type recombinant SWMb are essentially identical to results for native SWMb (Chance et al., 1984). We do, however, observe significant changes in the structures of the three mutant proteins MbL89D, MbL89I, and MbL89V. MbL89D at room temperature, where the sample is essentially in the aquo-met form, exhibits an LFIR ratio of 1.4. Although distortions in the heme such as doming and ruffling can significantly affect the LFIR parameter, an LFIR ratio of 1.4 corresponds to an Fe out-of-plane distance (Fe−ct) of ∼0.5 Å (Chance et al., 1984, 1986a).

An LFIR of 1.4 (0.5 Å) is very similar to the values for wt aquo-met myoglobin (Powers, 1989) but is also similar to values for some peroxidases such as ferric HRP and CcP (1.33, 0.5 Å (Chance et al., 1984, 1986a)). Upon freezing at ∼−75° or ∼−100 °C, the MbL89D LFIR ratio changes to 1.05, corresponding to an Fe−ct distance of ∼0.3 Å. Freezing at ∼−40 °C produces an apparent intermediate LFIR ratio of 1.15 (0.35 Å). The change in spin state upon freezing, identified by EPR spectroscopy, is behavior more typical of peroxidases than globins, and we suggest that these changes reflect the formation of a species similar to that observed for *A. ramosus* peroxidase (Farhangrazi et al., 1994; Powers et al., 1994; Powers, 1994) and lactoperoxidase (Chang et al., 1993). At these low temperatures, MbL89D has an average Fe−N_p of 1.985 Å, Fe−N_ϵ of 1.92 Å, and Fe−X of 2.08 Å. However, these results are significantly different at ∼−40 °C, with an average Fe−N_p of 2.02 Å, Fe−N_ϵ of 1.90 Å, and Fe−X dramatically changed to 2.35 Å. The large negative Debye−Waller factor (Table 2) associated with the Fe−X distance at this temperature indicates either large disorder of the distal ligand or an average structure of a population. As the decrease in temperature lengthens the average Fe−N_p and Fe−X distances, we can speculate that the room-temperature structure of MbL89D would have an extremely long or essentially unbound distal ligand and appear very similar to CcP. Our optical absorption data at room temperature show no indication of heterogenous populations and suggest a 5-coordinate species.

MbL89I and MbL89V mutants were constructed as controls. It is therefore surprising that we see differences between the XAS data of these proteins and wild type. While the LFIR parameters and Fe−N_p distances are essentially unchanged between the three proteins, MbL89V exhibits a significantly longer Fe−N_ϵ distance. Placing the Debye−Waller factors in order of decreasing disorder for the four globins, we find MbL89D to have the least disorder ($+8.2 \times 10^{-3}$ Å^{-2}) and MbL89V to exhibit the most disorder (-1.6×10^{-2} Å^{-2}). The disorder in the Fe−N_ϵ bond is due to two factors: the strength of the hydrogen bond holding it in place and the availability of space in which it can move. In wild type, there are two (weak) hydrogen bonds (from the backbone carbonyl of L89 and S92) holding the proximal histidine in place, and there is no space for movement. As a result, the Fe−N_ϵ distance is ordered, with a Debye−Waller factor of $+4.7 \times 10^{-3}$ Å^{-2}. Aspartic acid is slightly smaller than leucine (van der Waals volumes of 91 and 124 Å^3, respectively). If the D89 side chain remains in the same orientation as the L89 side chain, the backbone carbonyl could still hydrogen bond to N_δ. The slightly smaller side chain would result in more disorder, giving a more negative Debye−Waller factor associated with Fe−N_ϵ. However, the Debye−Waller factor increases by a factor of almost 2. This increase reflects a reduction in the disorder probably due to the shorter Fe−N_ϵ distance and stronger hydrogen bonding from D89 to H93 and provides evidence that the side-chain rotation observed in our computer modeling study may have occurred.

It is likely that rotation of the D89 side chain also results in disruption of the S92−H93 hydrogen bond due to local movement of the backbone. In MbL89D, the strength of the D89−H93 hydrogen bond more than compensates for this loss. However, in MbL89I and MbL89V, this is not the case. MbL89I is a very conservative substitution and would not be expected to be significantly different from wild

type. The Debye−Waller factor associated with the Fe−N_ϵ bond has, however, changed from the wild type value of $+4.7 \times 10^{-3}$ to -4.3×10^{-3} Å^{-2}, suggesting substantial disorder. This disorder is similar or greater in MbL89V with a Debye−Waller factor of -1.6×10^{-2} Å^{-2}. In a typical liquid, the Debye−Waller factor is $\sim -1 \times 10^{-2}$ Å^{-2}, leading to the concern that the proximal histidine may not be bonded in MbL89V. As the side chains of residue 89 in MbL89I and MbL89V are progressively smaller than leucine (L, 124 Å^3; I, 124 Å^3; V, 105 Å^3) and different shapes, we suggest that the increased pocket size allows for more movement of the proximal histidine in MbL89I and MbL89V. It is equally possible that the disorder we observe is a result of disruption of the S92−H93 hydrogen bond. The Fe−N_ϵ length of 2.28 Å in MbL89V probably therefore represents an almost unconstrained histidine.

Finally, the Soret peak shifts in the different proteins are as follows: Mb-N, 406 nm; MbL89I, 406 nm; MbL89V, 407 nm; and MbL89D, 413 nm. The Soret peak energy is affected by the overall electron density of the heme. We previously proposed (Sinclair et al., 1992) that increased hydrogen bonding to N_δ of the proximal ligand withdraws electron density from Fe−N_p via the proximal imidazole ring. If strong proximal hydrogen bonding withdraws electrons from the heme, we would expect lowering of the energy of the $\pi \rightarrow \pi^*$ transitions, resulting in a red-shifted Soret peak. In MbL89D, the Soret is indeed red shifted from 406 to 413 nm.

In summary, we have used XAS to investigate the structure of the iron heme environment in recombinant CcP and two mutants, CcPD235N and CcPW191F. CcPD235N exhibits a significantly lengthened Fe−N_ϵ bond, suggesting that the D235−H175 H-bond is responsible for the shorter (∼1.9 Å) Fe−N_ϵ bond in the peroxidases. Additionally, the longer Fe−N_ϵ bond in CcPD235N results in close coordination by a sixth ligand, possibly accompanied by distortion of the average heme plane. CcPW191F has a heme that is very similar to wt CcP. The unchanged Fe−N_ϵ bond length in this mutant provides further evidence that the D235−W191 H-bond largely serves to optimally position W191 for radical formation and electron transfer rather than to optimally position D235 for H-bonding with H175.

Conservative changes at myoglobin position 89, MbL89V and MbL89I, have profound consequences. Although the structure of the heme is not dramatically changed, disorder in the Fe−N_ϵ bond increases significantly as the size of the side chain decreases. This increased disorder has consequences for CN^- binding and possibly for other small ligands. Perhaps this is one reason for the near total conservation of leucine at position 89 in the globins. Substitution of aspartic acid at position 89 overcomes the increased disorder, presumably due to side chain rotation and strong D89−H93 hydrogen bonding. Despite several technical problems with the MbL89D sample preparation, peroxidase-like features were observed in MbL89D; most significantly, the Fe−N_ϵ bond is shortened in MbL89D by ∼0.20 Å. Other changes include a change in spin state upon freezing.

Overall, these results suggest that hydrogen bonding to the proximal histidine in the globins and peroxidases is largely responsible for the length of the Fe−N_ϵ bond. Elimination of the strong H-bond to N_δ in CcP in the mutant CcPD235N results in a change in Fe−N_ϵ from the typical peroxidase value of ∼1.9 Å to a globin-like distance of ∼2.1 Å. Conversely, introduction of strong proximal hydrogen bonding, presumably to N_δ, in the myoglobin mutant MbL89D, shortens Fe−N_ϵ from a typical globin-like distance to a peroxidase-like distance.

ACKNOWLEDGMENT

The authors thank Stephen C. Sligar for help and advice in preparing the Mb mutants, and Joseph Kraut and Mark M. Miller for generous donation of the CcP mutants and helpful discussions.

REFERENCES

Adachi, S., Nagano, S., Ishmori, K., Watanabe, Y., Morishima, I., Egawa, T., Kitagawa, T., & Makino, R. (1993) *Biochemistry 32*, 241−252.

Chance, B., Powers, L., Ching, Y., Poulos, T., Schonbaum, G. R., Yamazaki, Y., & Paul, G. K. (1984) *Arch. Biochem. Biophys. 235*, 596−611.

Chance, M., Parkhurst, L., Powers, L., & Chance, B. (1986a) *J. Biol. Chem. 261*, 5689−5692.

Chance, M., Powers, L., Kumar, C., & Chance, B. (1986b) *Biochemistry 25*, 1259−1265.

Chang, C. S., Yamazaki, I., Sinclair, R., Khalid, S., & Powers, L. (1993a) *Biochemistry 32*, 923−928.

Chang, C. S., Sinclair, R., Khalid, S., Yamazaki, I., Nakamura, S., & Powers, L. (1993b) *Biochemistry 32*, 2780−2786.

Collins, D., Countryman, R., & Hoard, J. (1972) *J. Am. Chem. Soc. 94*, 2066−2072.

Davies, M. (1990) *Free Radical Res. Commun. 10*, 361−370.

Davies, M. (1991) *Biochem. Biophys. Acta 1077*, 86−90.

deRopp, J. S., Thanabal, V., & LaMar, G. N. (1985) *J. Am. Chem. Soc. 107*, 8268−8270.

Evans, S., & Breyer, G. (1990) *J. Mol. Biol. 213*, 885−897.

Fenna, R., Zeng, J., & Davey, C. (1995) *Arch. Biochem. Biophys. 316*, 653−656.

Finzel, B. C., Poulos, T. L., & Kraut, J. (1984) *J. Biol. Chem. 259*, 13027−13036.

Fishel, L. A., Farnum, M. F., Mauro, J. M., Miller, M. A., Kraut, J., Liu, Y., Tan, X-l., & Scholes, C. P. (1991) *Biochemistry 30*, 1986−1996.

Fujita, I., Hanson, L. K., Walker, F. A., & Fajer, J. (1983) *J. Am. Chem. Soc. 105*, 3296−3300.

George, P., & Irvine, D. H. (1952) *Biochem. J. 52*, 511−517.

George, P., & Irvine, D. H. (1953) *Biochem. J. 55*, 230−236.

Goodin, D. B., & McRee, D. E. (1993) *Biochemistry 32*, 3313−3324.

Guillemette, J. G., Matsushima-Hibiya, Y., Atkinson, T., & Smith, M. (1991) *Protein Eng. 4*, 585−592.

Harada, K., & Yamazaki, I. (1987) *J. Biochem. 101*, 283−286.

Henrissat, B., Saloheimo, M., Lavaitte, S., & Knowles, J. K. C. (1990) *Proteins: Struct. Funct. Genet. 8*, 251−257.

Higuchi, R., Krummel, B., & Saiki, R. (1988) *Nucleic Acids Res. 16*, 7351−7367.

Houseman, A. L. P., Doan, P. E., Goodin, D. B., & Hoffman, B. M. (1993) *Biochemistry 32*, 4430−4443.

Iball, J., & Morgan, C. (1976) *Acta Crystallogr. B 23*, 239−244.

Khalid, S., Rosenbaum, G., & Chance, B. (1986) *Proc. SPIE Int. Soc. Opt. Eng. 690*, 65−67.

King, N. K., & Winfield, M. E. (1963) *J. Biol. Chem. 238*, 1520−1528.

Kunishima, N., Fukuyama, K., Matsubara, H., Hatanaka, H., Shibano, Y., & Amachi, T. (1994) *J. Mol. Biol. 235*, 331−344.

LaMar, G. N., & deRopp, J. S. (1982) *J. Am. Chem. Soc. 104*, 5203−5206.

Lee, P., Citrin, P., Eisenberger, P., & Kincaid, B. (1981) *Rev. Mod. Phys. 53*, 769−806.

Lionetti, C., Guanziroli, M. G., Frigerio, F., Ascenzi, P., & Bolognesi, M. (1991) *J. Mol. Biol. 217*, 409−412.

Miki, H., Harada, K., Yamazaki, I., Tamura, M., & Watanabe, H. (1989) *Arch. Biochem. Biophys. 275*, 354−362.

Mincey, T., & Traylor, T. G. (1979) *J. Am. Chem. Soc. 101*, 765−770.
Peisach, J. (1975) *Ann. N.Y. Acad. Sci. 244*, 187−200.
Peisach, J., Powers, L., Blumberg, W. E., & Chance, B. (1982) *Biophys. J. 38*, 227−285.
Pelletier, H., & Kraut, J. (1992) *Science 258*, 1748−1755.
Poulos, T. L., & Kraut, J. (1980) *J. Biol. Chem. 255*, 8199−8205.
Poulos, T. L., & Finzel, B. C. (1984) *Pept. Protein Rev. 4*, 115−171.
Poulos, T., Edwards, S., Wariishi, H., & Gold, M. (1993) *J. Biol. Chem. 268*, 4429−4440.
Powers, L. (1989) in *Proceedings, Fine Particle Society, Forrest Carter Memorial Symposia* (Hong, F., Ed.) p 115, Plenum Publishers, New York.
Powers, L. (1994) *Molecular Electronics and Molecular Electronic Devices*, Vol. 3, pp 211−222, CRC Press Inc., Boca Raton, FL.
Powers, L., & Kincaid, B. (1989) *Biochemistry 28*, 4461−4468.
Powers, L., Chance, B., Ching, Y., & Angiolillo, P. (1981) *Biophys. J. 34*, 465−498.
Powers, L., Sessler, J. S., Woolery, G. L., & Chance, B. (1984) *Biochemistry 23*, 5519−5523.
Powers, L., Chance, B., Chance, M., Campbell, B., Friedman, J., Khalid, S., Kumar, C., Naqui, A., Reddy, K. S., & Zhou, Y. (1987) *Biochemistry 26*, 4785−4796.
Powers, L., Sinclair, R., Chance, B., Reddy, K. S., & Yamazaki, I. (1994) in *Synchrotron Radiation in the Biosciences* (Chance, B., Deisenhofer, J., Ebashi, S., Goodhead, D., Helliwell, J., Huxley, H., Iizuka, T., Kirz, J., Mitsui, T., Rubenstein, E., Sakabe, N., Sasaki, T., Schmahl, G., Stuhrmann, H., Wuthrich, K., & Zaccai, G., Eds.) pp 302, 312, Clarendon Press, New York.
Reddy, K. S., Powers, L. Lee, C., & Chance, B. (1992) *Biophys. J. 61*, A214.
Sambrook, J., Fritsch, E. F., & Maniatis, T. (1989) *Molecular Cloning. A Laboratory Manual*, Cold Spring Harbor Laboratory Press, Cold Spring Harbor, NY.
Satterlee, J., Erman, J., Mauro, J., & Kraut, J. (1990) *Biochemistry 29*, 8797−8804.
Schuller, D., Ban, N., van Huystee, R., McPherson, A., & Poulos, T. (1996) *Structure 4*, 311−321.
Sinclair, R., Yamazaki, I., Bumpus, J., Brock, B., Chang, C.-S., Albo, A., & Powers, L. (1992) *Biochemistry 31*, 4892−4900.
Sinclair, R. Copeland, B., Yamazaki, I., & Powers, L. (1995) *Biochemistry 34*, 13176−13182.
Sivaraja, M., Goodin, D., Smith, M., & Hoffman, B. (1989) *Science 245*, 738−740.
Smerdon, S. J., Krzywda, S., Wilsonson, A. J., Brantley, R. E., Jr., Carver, T. E., Hargrove, M. S., & Olson, J. S. (1993) *Biochemistry 32*, 5132−5138.
Smulevich, G., Mauro, J. M., Fishel, L. A., English, A. M., Kraut, J., & Spiro, T. G. (1988a) *Biochemistry 27*, 5477−5485.
Smulevich, G., Mauro, J. M., Fishel, L. A., English, A. M., Kraut, J., & Spiro, T. G. (1988b) *Biochemistry 27*, 5486−5492.
Smulevich, G., Mantini, A., English, A., & Mauro, J. (1989) *Biochemistry 28*, 5058−5064.
Smulevich, G., Wang, Y., Edwards, S. L., Poulos, T. L., English, A. M., & Spiro, T. G. (1990a) *Biochemistry 29*, 2586−2592.
Smulevich, G., Wang, Y., Mauro, J. M., Wang, J., Fishel, L. A., Kraut, J., & Spiro, T. G. (1990b) *Biochemistry 29*, 7174−7180.
Smulevich, G., Miller, M. A., Kraut, J., & Spiro, T. G. (1991) *Biochemistry 30*, 9546−9558.
Springer, B. A., & Sligar, S. G. (1987) *Proc. Natl. Acad. Sci. U.S.A. 84*, 8961−8965.
Stayton, P. S., Atkins, W. M., Springer, B. A., & Sligar, S. G. (1989) *Met. Ions Biol. Syst. 25*, 417−475.
Tang, H.-L., Chance, B., Mauk, A., Powers, L., Reddy, K. S., & Smith, M. (1994) *Biochim. Biophys. Acta 1206*, 90−96.
Tew, D., & Ortiz de Montellano, P. R. (1988) *J. Biol. Chem. 263*, 17880−17886.
Traylor, T. G., & Popovitz-Biro, R. (1988) *J. Am. Chem. Soc. 110*, 239−243.
Valentine, J., Sheridan, R., Allen, L., & Kahn, P. (1979) *Proc. Natl Acad. Sci. U.S.A. 76*, 1009−1013.
Vitello, L., Erman, J., Miller, M., Mauro, J., & Kraut, J. (1992) *Biochemistry 31*, 11524−11535.
Wang, J., Mauro, J. M., Edwards, S. L., Oatley, S. J., Fishel, L. A., Ashford, V. A., Xuong, N., & Kraut, J. (1990) *Biochemistry 29*, 7160−7173.
Yonetani, T. (1965) *J. Biol. Chem. 240*, 4509−4514.
Yonetani, T. (1970) *Adv. Enzymol. 33*, 309−335.
Yonetani, T., & Schleyer, H. (1967) *J. Biol. Chem. 242*, 1974−1979.
Yonetani, T., Chance, B., & Kajiwara, S. (1966a) *J. Biol. Chem. 241*, 2981−2986.
Yonetani, T., Schleyer, H., & Ehrenberg, A. (1966b) *J. Biol. Chem. 241*, 3240−3243.

BI961064I